Strong dissipation of steep swells observed across oceans

Fabrice Ardhuin, Bertrand Chapron, Fabrice Collard

Strong dissipation of steep swells observed across oceans

Fabrice Ardhuin

Service Hydrographique et Océanographique de la Marine, Brest, France

Bertrand Chapron

Laboratoire d'Océanographie Spatiale, Ifremer, Centre de Brest, Plouzané, France

Fabrice Collard

Collecte Localisation Satellites, division Radar, Plouzané, France

Global observations of ocean swell propagation is presented and analyzed, using on four years of satellite Synthetic Aperture Radar data. Tracking swells along their propagation paths yields an estimation of the dissipation of their energy. Swells can be very persistent with energy e-folding scales exceeding 30,000 km. For increasing swell steepness, this scale shrinks down to 2700 km, revealing a significant loss of swell energy. This pattern is consistent with a laminar to turbulent transition of the boundary layer, induced by the opposite wave-induced motions of air and water, with a threshold Reynolds number of the order of 100,000. This finding opens the way for more accurate wave forecasting models, and provides a constraint on swell-induced air-sea fluxes of momentum and energy.

1. Introduction

Swells are surface waves that outrun their generating wind, and radiate across ocean basins. Wind-waves that radiate away from their generation area dissipate and grow in length over a relatively short distance[*Snodgrass et al.*, 1966], say 2000 km. Further away, these waves closely follow principles of geometrical optics, with a constant wave period along geodesics, when following a wave packet at the group speed[e.g. *Snodgrass et al.*, 1966]. These geodesics are great circles along the Earth surface, with minor deviations due to ocean currents. As it takes a longer fetch or a faster wind to develop higher and longer waves, swells recorded by in situ measurements have been used to estimate the positions and intensity of generating storms across the oceans [*Munk and Snodgrass*, 1957].

Because swells are observed to propagate over long distances, their energy should be conserved or weakly dissipated[*Snodgrass et al.*, 1966], but little quantitative information is available on this topic. Due to this poor knowledge, swells are relatively poorly predicted. Numerical wave models that neither account specifically for swell dissipation, nor assimilate wave measurements, invariably overestimate significant wave heights (H_s) in the tropics. Typical biases in such models reach 45 cm or 25% of the mean observed wave height in the East Pacific [*Rascle et al.*, 2008]. Further, modelled peak periods along the North American west coast exceed those measured by open ocean buoys, on average by 0.8 s [*Rascle et al.*, 2008], indicating an excess of long period swell energy. Previously proposed swell dissipation parameterizations, [e.g. *Tolman*, 2002], on the contrary lead to underestimations, up to 0.8 s, of peak periods in the Pacific. Swell evolution over large scales is thus not understood.

Swells are also observed to modify air-sea interactions [*Grachev and Fairall*, 2001], and it swell energy has been suggested as a possible source of ocean mixing [*Babanin*, 2006]. A quantitative knowledge of the swell energy budget is thus needed both for marine weather forecasting and Earth system modelling.

The only experiment that followed swell evolution at oceanic scales was carried out in 1963. Using in situ measurements, a very uncertain but moderate dissipation of wave energy was found [*Snodgrass et al.*, 1966]. The difficulty of this type of analysis are twofold. First, very few storms produce swells that line up with any measurement array, and second, large errors are introduced by having to account for island sheltering. Qualitative investigations by *Holt et al.* [1998] and *Heimbach and Hasselmann* [2000] demonstrated that a space-borne synthetic aperture radar (SAR) could be used to track swells across the ocean, building on the coherent persistence of swells along their propagation tracks. Here we make a quantitative analysis of four years of global SAR measurements, using level 2 wave spectra [*Chapron et al.*, 2001] from the European Space Agency's (ESA) ENVISAT satellite. The swell analysis method is presented in section 2. The resulting estimates of swell dissipation are interpreted in section 3, and conclusions follow in section 4.

2. Swell tracking and dissipation estimates

Our analysis uses a two step method. Firstly, using SAR-measured wave periods and directions at different times and locations, we follow great circle trajectories backwards at the theoretical group velocity. The location and date of swell sources is defined as the spatial and temporal center of the convergence area and time of the trajectories. Figure 1 illustrates this first step with a swell covering one Earth quadrant away from the storm, except for a large detection gap from the Southern Pacific to California. This blank area is the long shadow cast by French Polynesia where wave energy is dissipated in the surf [e.g. *Tolman*, 2003].

Secondly, we track the swells forward in space and time, starting from the source at an angle θ_0, and following ideal geodesic paths in search of SAR observations. Great circle tracks are traced from the source in all directions, except for angular sectors with islands. Along each track, SAR data are selected if they are acquired within 3 hours and 100 km from the theoretical position. In a first filtering procedure, we retain only SAR-derived swell partitions with peak wavelength and direction within 50 m and 20° of their theoretical values when assuming a point source. Tracks with neighboring values of the outgoing direction θ_0 were merged in relatively narrow direction bands (5 to 10° aperture) in order to increase the number of observations along a track, yielding 29 track ensembles.

If no energy is lost by the wave field, the spectral density $F(f, \theta, \varphi, \theta_0)$ is constant along the propagation path, where

0094-8276/08/$5.00

$f = 1/T$ is the wave frequency, θ is the local wave propagation direction, and φ is the separation angle, from the source, on the spherical Earth. A stationary storm that generates a broad wave spectrum yields a swell energy per unit ocean surface $E_s(\varphi,\theta_0) = \int\int F(f,\theta,\varphi,\theta_0)\mathrm{d}f\mathrm{d}\theta$, in which the integration is over the swell partition only. E_s decreases asymptotically as $1/[\varphi\sin(\varphi)]$ away from the source[*Munk et al.*, 1963, see also auxiliary information, discussion 2]. The $\sin(\varphi)$ factor arises from the initial spatial expansion of the energy front, with a narrowing of the directional spectrum. The φ factor is due to the dispersive spreading of the energy packet, because the group speed C_g is inversely proportional to the wave period, associated to a narrowing of the the frequency spectrum In each track ensemble, all swells have close initial directions θ_0, and the wave field is only a function of φ. We define the spatial evolution rate

$$\alpha = -\frac{\mathrm{d}F(f,\theta,\varphi)/\mathrm{d}\varphi}{RF(f,\theta,\varphi)}, \qquad (1)$$

where R is the Earth radius. Positive values of α correspond to losses of wave energy (Figure 2.b).

The swell dissipation scale was then estimated by finding the constant value of α, defined in eq. (3), that minimized the difference between theoretical and observed swell height decays. In each ensemble, some SAR data were filtered out (see 'Methods' in auxiliary information): This removed all the data within 4000 km of the originating storm to make sure that the remaining data are in the far field of the storm, where, in the absence of dissipation, the energy decays asymptotically as $1/[\varphi sin(\varphi)]$.

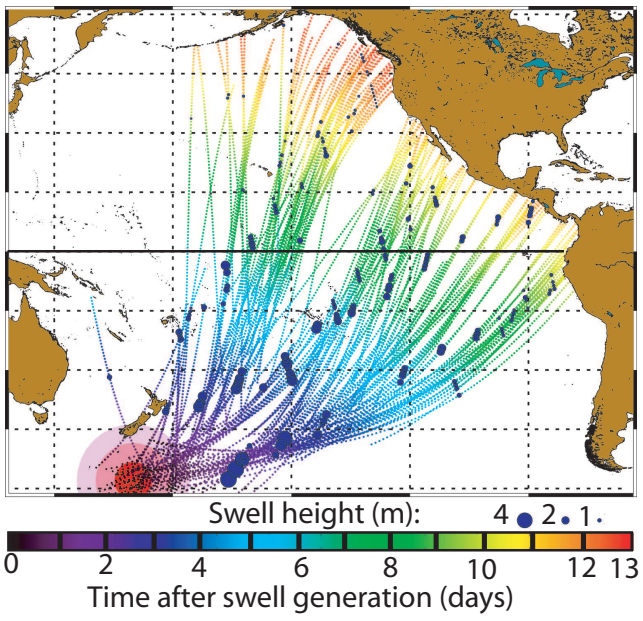

Figure 1. Finding the source storm. All swells with a 17 ± 0.5 s period that were identified in 13 days of ENVISAT synthetic aperture radar data over the Pacific, are re-focussed from their location of observation (filled dots) following their direction of arrival at the theoretical group speed for 17 s waves. This focussing reveals a single swell generation event, well defined in space and time (pink to red disks). The back-tracking trajectories are color-dated from black (July 9 2004 18:00 UTC) to red (July 22 2004 18:00 UTC).

We estimate that the SAR-derived swell heights $H_{ss} = 4\sqrt{E_s}$ are gamma-distributed about the true value μ with bias

$$\langle H_{ss}\rangle - \mu = 0.1H_{ss} - 0.15\max\{0, U_{10} - 7\} \qquad (2)$$

where H_{ss} in meters and the wind speed U_{10} is in m s^{-1}, and a standard deviation given by

$$\sigma = \max\{0.15, \min\{0.25H_{ss}, 0.4\}\} \qquad (3)$$

where σ and H_{ss} are in meters (auxiliary information, discussion 3). Using this error model, we generated 400 synthetic data sets in which each measured swell wave heights were perturbed independently, in order to estimate errors on α. Similarly, a non-linear dissipation function with a constant value of the dissipation factor f_e (eq. 5) was also fitted

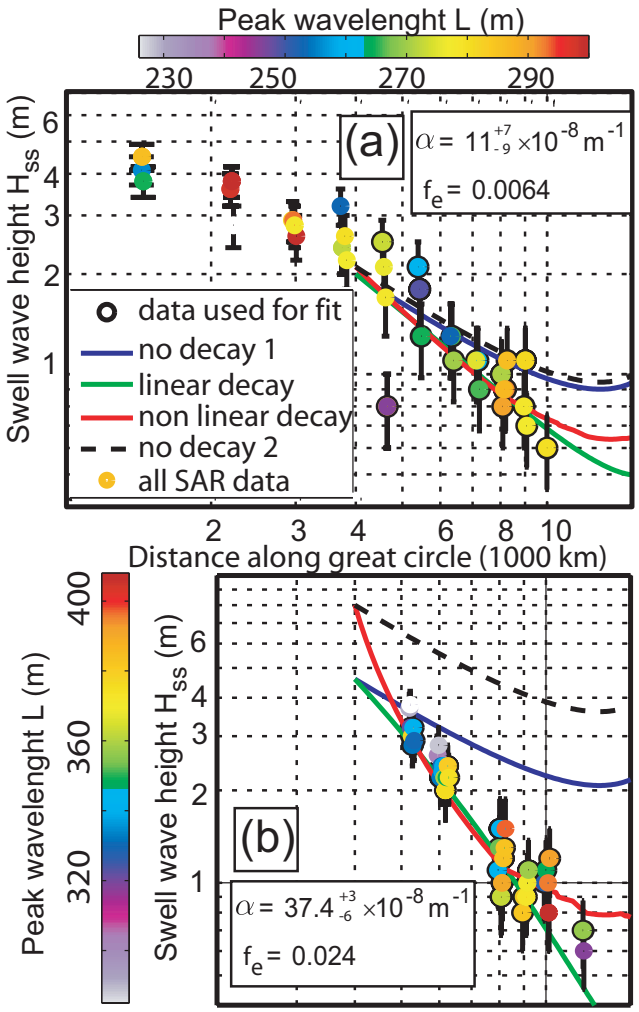

Figure 2. (a) Observed swell wave height as a function of distance, and theoretical decays with fitted coefficients using no dissipation, linear or non-linear dissipation, for the 13 s waves generated by Typhoon Ting-Ting. Circled dots are the observations used in the fitting procedure. Error bars show one standard deviation of the expected error on each SAR measurement (auxiliary information discussion 2) . (b), Same as (a) for steeper swells observed in February 2007.

to the data, using a numerical wave model (see auxiliary information).

For all or swell data, α ranges from -0.6 to 3.7 $\times$ 10^{-7} m^{-1} (Figure 3.a), comparable to 2.0×10^{-7} m^{-1} previously reported for large amplitude swells with a 13 s period[*Snodgrass et al.*, 1966]. Clarifying earlier observations by *Darbyshire* [1958] and *Snodgrass et al.* [1966], our analysis unambiguously proves that swell dissipation increases with the wave steepness.

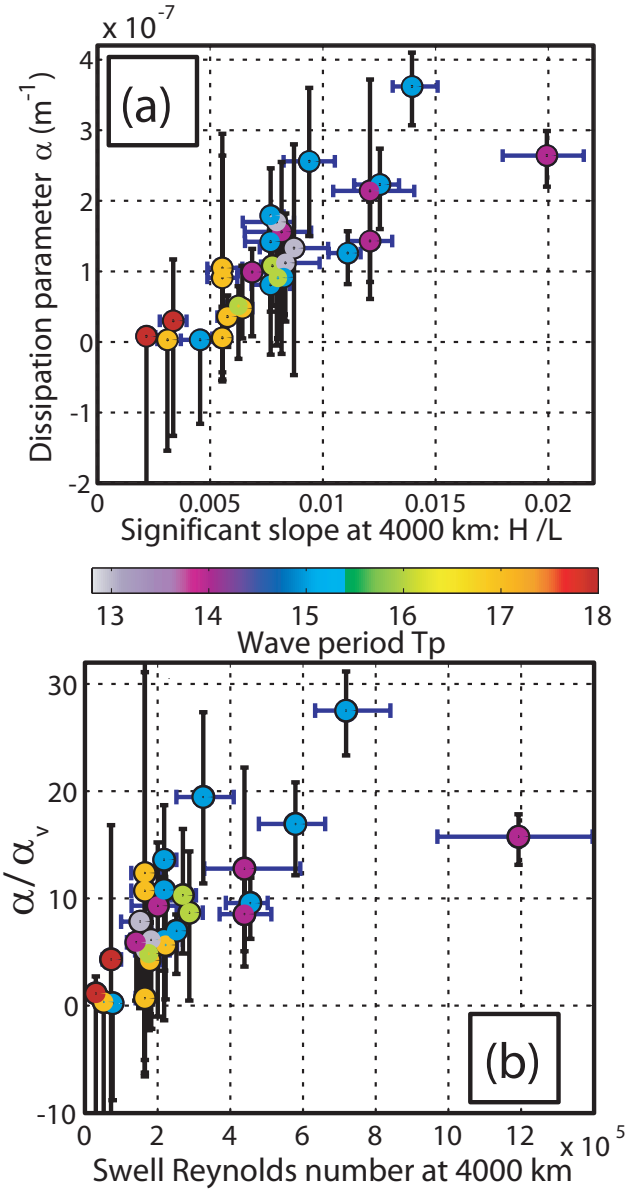

Figure 3. Swell dissipation for 29 events. (a) Estimated linear attenuation coefficient as a function of the initial significant slope, ratio of the significant wave height and the peak wavelength, $s = 4H_s/L$, taken 4000 km from the storm centre, for a variety of peak swell periods (colors). (b) Attenuation coefficient normalized by the viscous attenuation α_ν (eq. 2), as a function of the swell Reynolds number Re_s determined from r.m.s. velocity and displacement amplitudes at 4000 km from the storm.

3. Interpretation of swell dissipation

At present there is no consensus on the plausible causes of the loss of swell energy [*WISE Group*, 2007]. Interaction with oceanic turbulence is expected to be relatively small [*Ardhuin and Jenkins*, 2006]. Observed modifications and reversals of the wind stress over swells [*Grachev and Fairall*, 2001] suggest that some swell momentum is lost to the atmosphere. The wave-induced modulations of stresses yield a flux of energy from the waves to the wind, due to the correlations of pressure and velocity normal to the sea surface, and the correlations of shear stress and tangential velocity. Both can yield an upward flux of momentum, readily observed over steep laboratory waves, in the form of a wave-driven wind [*Harris*, 1966]. In recent models of airflows over waves, these modulations have been linearized [e.g. *Kudryavtsev and Makin*, 2004], so that the swell dissipation rate is linear in terms of the wave energy, and cannot increase with the swell steepness.

Because our observation show no clear trend with wind magnitude and direction, we take a novel approach, and interpret our data by neglecting the effect of the wind, considering only the shear stress modulations induced by swell orbital velocities. Little data is available for air flows over swells, but boundary layers over fixed surfaces are well known, and should have similar properties if their significant orbital amplitudes of velocity and displacement are doubled (see auxiliary information discussion 4). The flow should thus depend on the surface roughness and a significant Reynolds numbers, $\mathrm{Re}(\varphi) = 4u_{\mathrm{orb}}(\varphi)a_{\mathrm{orb}}(\varphi)/\nu$.

For $\mathrm{Re} < 10^5$, the flow should be laminar [*Jensen et al.*, 1989]. Due to the strong shear above the surface, the air viscosity is important, with a dissipation coefficient given by *Dore* [1978]

$$\alpha_\nu = 2\frac{\rho_a 2\pi}{\rho_w C_g L}\sqrt{4\pi\nu/T}, \qquad (4)$$

where L is the swell wavelength, $L = gT^2/(2\pi)$ in deep water with g the acceleration of gravity. At ambient temperature and pressure, the air viscosity is $\nu = 1.4\times10^{-5}$ m^2s^{-1}, and α_ν is only a function of T. As T increases from 13 to 19 s, α_ν decreases from 2.2×10^{-8} to $5.8\times10^{-9}m^{-1}$.

For larger Reynolds number the flow should be turbulent. Following common practice, the energy rate of decay in time is

$$\beta = C_g\alpha = \frac{\rho_a 4\pi^2}{\rho_w g T^2} f_e u_{\mathrm{orb}} \qquad (5)$$

where f_e is a swell dissipation factor, of the order of 0.002 to 0.008 for a smooth surface[*Jensen et al.*, 1989], when f_e is assumed equal to the friction factor f_w.

Re is difficult to estimate from the SAR data only, because ENVISAT's ASAR does not resolve the short windsea waves. However, in deep water we can define the smaller 'swell Reynolds number' Re_s from $u_{\mathrm{orb,s}} = 2\sqrt{E_s}2\pi/T$ and $a_{\mathrm{orb,s}} = 2\sqrt{E_s}$. For reference, a 6.3 m s^{-1} wind generates short waves with $\mathrm{Re}= 2\times10^5$, making the boundary layer turbulent for any swell amplitude.

Our estimates of α exceed α_ν by a factor that ranges from $O(1)$ to 28 (Figure 3.b). Our results thus presents quantitative similarities with oscillatory boundary layer over fixed surfaces with no or little roughness. Namely, dissipation rates α of the order of the viscous value α_ν are found for $\mathrm{Re}_s < 5\times10^4$ when the the flow may be laminar, and we only find large values of α/α_ν when $\mathrm{Re}_s > 5\times10^4$ over a significant portion of the swell track (figure 3.b). Using a numerical wave model, this value of Re_s translates to $\mathrm{Re}\simeq 10^5$.

Using modelled values of $u_{\rm orb}$ and fitting a constant f_e for each set of observations, yields $0.001 \leq fe \leq 0.024$, with a median of 0.009, close to what is expected over a smooth surface. A simple parameterization of swell dissipation, taking f_e constant at 0.0035, generally yields accurate wave heights (see Auxiliary Information, discussion 5).

Intuitively, winds should modify the boundary layer over swell, but may only dominate for winds larger than 7 m s^{-1} (auxiliary information discussion 4). *Kudryavtsev and Makin* [2002] considered the wind stress modulations due to short wave roughness modulated by swells, and found. Yet, their linear model cannot explain the nonlinear dissipation observed here, because they only considered lowest order effects. Further investigations should probabably consider both wind and finite amplitude swell effects to explain the observed variability of α.

If this dissipation is due to the proposed air-sea friction mechanism, the associated momentum flux $\rho_w g E_s/2$ goes to the atmosphere. If underwater processes are involved, an energy flux $\rho_w g C_g E_s$ may go into ocean turbulence. Accordingly, these fluxes are small. For 3 m high swells, the momentum flux is only 8% of the wind stress produced by a 3 m s^{-1} wind. This momentum flux thus plays a minor role in observed O(50%) modifications of the wind stress at low wind[*Grachev and Fairall*, 2001]. Wind stress modifications are more likely related to a nonlinear influence of swell on turbulence in the atmospheric boundary layer [*Sullivan et al.*, 2008]. The dissipation coefficient α is a key parameter for models of this effect [*Kudryavtsev and Makin*, 2004; *Hanley and Belcher*, 2008].

4. Conclusions

Using high quality data from a space-borne synthetic aperture radar, ocean swells of periods 13 to 18 s were systematically tracked across ocean basins over the period 2003 to 2007. Among these, 12 storms provided enough data to allow a a total of 28 estimations of the swell energy budget. The dissipation of small-amplitude swells is not distinguishable from viscous dissipation, with decay scales larger than 30000 km. On the contrary, steep swells lose a significant fraction of their energy, up to 65% over a distance as short as 2700 km. This non-linear behavior is consistent with a transition from a laminar to a turbulent air-side boundary layer. The present analysis opens the way for a better understanding of air-sea fluxes in low wind conditions. A satisfactory parameterization of this swell dissipation [*Ardhuin et al.*, 2008] was introduced in May 2008 in the global-scale wave forecasting research system operated by SHOM. Without wave data assimilation, this system still provides forecasts for swell-dominated regions, such as the U.S. West coast or North-West Australia, that are significantly more accurate in terms of wave heights than the operational systems developed earlier (see http://www.jcomm-services.org/Wave-Forecast-Verification-Project.html). Further investigations are necessary to understand the wind stress modulations and its variation with wind speed, direction, and swell amplitude. Such an effort is essential for the further improvement of numerical wave models.

Acknowledgments. SAR data was provided by the European Space Agency (ESA). The swell decay analysis was funded by the French Navy as part of the EPEL program. This work is a contribution to the ANR-funded project HEXECO and DGA-funded project ECORS.

References

Ardhuin, F., and A. D. Jenkins (2006), On the interaction of surface waves and upper ocean turbulence, *J. Phys. Oceanogr.*, *36*(3), 551–557.

Ardhuin, F., F. Collard, B. Chapron, P. Queffeulou, J.-F. Filipot, and M. Hamon (2008), Spectral wave dissipation based on observations: a global validation, in *Proceedings of Chinese-German Joint Symposium on Hydraulics and Ocean Engineering, Darmstadt, Germany*.

Babanin, A. V. (2006), On a wave-induced turbulence and a wave-mixed upper ocean layer, *Geophys. Res. Lett.*, *33*(3), L20,605, doi:10.1029/2006GL027308.

Chapron, B., H. Johnsen, and R. Garello (2001), Wave and wind retrieval from SAR images of the ocean, *Ann. Telecommun.*, *56*, 682–699.

Darbyshire, J. (1958), The generation of waves by wind, *Phil. Trans. Roy. Soc. London A*, *215*(1122), 299–428.

Dore, B. D. (1978), Some effects of the air-water interface on gravity waves, *Geophys. Astrophys. Fluid. Dyn.*, *10*, 215–230.

Grachev, A. A., and C. W. Fairall (2001), Upward momentum transfer in the marine boundary layer, *J. Phys. Oceanogr.*, *31*, 1698–1711.

Hanley, K. E., and S. E. Belcher (2008), Wave-driven wind jets in the marine atmospheric boundary layer, *J. Atmos. Sci.*, *65*, 2646–2660.

Harris, D. L. (1966), The wave-driven wind, *J. Atmos. Sci.*, *23*, 688–693.

Heimbach, P., and K. Hasselmann (2000), Development and application of satellite retrievals of ocean wave spectra, in *Satellites, oceanography and society*, edited by D. Halpern, pp. 5–33, Elsevier, Amsterdam.

Holt, B., A. K. Liu, D. W. Wang, A. Gnanadesikan, and H. S. Chen (1998), Tracking storm-generated waves in the northeast pacific ocean with ERS-1 synthetic aperture radar imagery and buoys, *J. Geophys. Res.*, *103*(C4), 7917–7929.

Jensen, B. L., B. M. Sumer, and J. Fredsøe (1989), Turbulent oscillatory boundary layers at high Reynolds numbers, *J. Fluid Mech.*, *206*, 265–297.

Kudryavtsev, V. N., and V. K. Makin (2002), Coupled dynamics of short waves and the airflow over long surface waves, *J. Geophys. Res.*, *107*(C12), 3209, doi:10.1029/2001JC001251.

Kudryavtsev, V. N., and V. K. Makin (2004), Impact of swell on the marine atmospheric boundary layer, *J. Phys. Oceanogr.*, *34*, 934–949.

Munk, W. H., and F. E. Snodgrass (1957), Measurements of southern swell at Guadalupe island, *Deep Sea Res.*, *4*, 272–286.

Munk, W. H., G. R. Miller, F. E. Snodgrass, and N. F. Barber (1963), Directional recording of swell from distant storms, *Phil. Trans. Roy. Soc. London A*, *255*, 505–584.

Rascle, N., F. Ardhuin, P. Queffeulou, and D. Croizé-Fillon (2008), A global wave parameter database for geophysical applications. part 1: wave-current-turbulence interaction parameters for the open ocean based on traditional parameterizations, *Ocean Modelling*, doi:10.1016/j.ocemod.2008.07.006.

Snodgrass, F. E., G. W. Groves, K. Hasselmann, G. R. Miller, W. H. Munk, and W. H. Powers (1966), Propagation of ocean swell across the Pacific, *Phil. Trans. Roy. Soc. London*, *A249*, 431–497.

Sullivan, P. P., J. B. Edson, T. Hristov, and J. C. McWilliams (2008), Large-eddy simulations and observations of atmospheric marine boundary layers above nonequilibrium surface waves, *J. Atmos. Sci.*, *65*(3), 1225–1244.

Tolman, H. L. (2002), Validation of WAVEWATCH-III version 1.15, *Tech. Rep. 213*, NOAA/NWS/NCEP/MMAB.

Tolman, H. L. (2003), Treatment of unresolved islands and ice in wind wave models, *Ocean Modelling*, *5*, 219–231.

WISE Group (2007), Wave modelling the state of the art, *Progress in Oceanography*, *75*, 603–674, doi: 10.1016/j.pocean.2007.05.005.

Fabrice Ardhuin, Service Hydrographique et Océanographique de la Marine, 29609 Brest, France. (ardhuin@shom.fr)

Bertrand Chapron, Laboratoire d'Océanographie Spatiale, Ifremer, Centre de Brest, 29280 Plouzané, France. (bertrand.chapron@ifremer.fr

Fabrice Collard, Collecte Localisation Satellites, division Radar, 29280 Plouzané, France. (Dr.fab@cls.fr)